



On the onset of deformation twinning in the CrFeMnCoNi high-entropy alloy using a novel tensile specimen geometry

Keli V.S. Thurston^{a,b}, Anton Hohenwarter^c, Guillaume Laplanche^d, Easo P. George^{e,f}, Bernd Gludovatz^{g,*}, Robert O. Ritchie^{a,b,**}

^a Materials Sciences Division, Lawrence Berkeley National Laboratory, Berkeley, CA 94720, USA

^b Department of Materials Science & Engineering, University of California, Berkeley, CA 94720, USA

^c Department of Materials Science, Chair of Materials Physics, Montanuniversität Leoben and Erich Schmid Institute of Materials Science, Austrian Academy of Sciences, A-8700 Leoben, Austria

^d Institut für Werkstoffe, Ruhr-Universität Bochum, D-44780 Bochum, Germany

^e Materials Science & Technology Division, Oak Ridge National Laboratory, Oak Ridge, TN 37831, USA

^f Materials Science & Engineering Department, University of Tennessee, Knoxville, TN 37996, USA

^g School of Mechanical and Manufacturing Engineering, UNSW Sydney, NSW 2052, Australia

ARTICLE INFO

Keywords:

High-entropy alloy
Cantor alloy
Deformation twinning
Twinning stress
Critical twinning strain

ABSTRACT

Deformation-induced nanoscale twinning is one of the mechanisms responsible for the excellent combination of strength and fracture toughness of the single-phase, face-centered cubic CrMnFeCoNi (Cantor) alloy, especially at cryogenic temperatures. Here, we use a novel, modified dogbone geometry that permits the sampling of varying stress and strain regions within a single tensile specimen to characterize the onset of twinning in CrMnFeCoNi at 293 K, 198 K and 77 K. Electron backscatter diffraction (EBSD) and backscattered electron (BSE) imaging revealed the presence of deformation nano-twins in regions of the samples that had experienced plastic strains of ~25% at 293 K, ~16% at 198 K, and ~8% at 77 K, which are similar to the threshold strains described by Laplanche et al. (*Acta Mater.* 118, 2016, 152–163). From these strains we estimate that the critical tensile stress for the onset of twinning in this alloy is on the order of 750 MPa.

1. Introduction

The near-equiatomic family of high-entropy alloys (HEAs) represent a rapidly growing branch of metals and material design that holds great potential due to their variety of unusual compositional and microstructural characteristics combined with promising mechanical properties. The best-known example of this class of alloys, the so-called ‘Cantor’ alloy (CrMnFeCoNi) [1], has drawn particular interest because of its excellent combination of strength, ductility and fracture toughness [2–6], all of which improve at cryogenic temperatures. This absence of the conventional strength-toughness tradeoff has been observed in relatively few materials classes, although one such class is twinning-induced plasticity, or ‘TWIP’, steels [7–9] which display a similar temperature dependence of mechanical properties with both strength and toughness improving with decreasing temperature [8,10,11]. In both CrCoNi-based HEAs and TWIP steels, deformation

twinning can significantly contribute to the hardening of the materials [8]. In the Cantor alloy, the transition from dislocation glide to deformation twinning is associated with a relatively low stacking fault energy (SFE) [12] that additionally requires sub-zero temperatures [3] and/or higher stresses to be activated [13,14]. These deformation characteristics are similar to those of its related medium-entropy alloy CrCoNi, particularly noting the coincidence of deformation twinning with the excellent mechanical behavior at lower temperatures [3,6,15,16].

Recent work by Laplanche et al. [17] utilized the carefully performed transmission electron microscopy (TEM) studies performed by Otto et al. [3] to specify the onset strains of nano-twinning and the corresponding critical resolved shear stresses in the Cantor alloy at 293 K and 77 K. Specifically, they found that decreasing the temperature from 293 K to 77 K led to a decrease in the true strain for the onset of deformation twinning, from 25% to 7.4%, while the corre-

* Corresponding author.

** Corresponding author. Materials Sciences Division, Lawrence Berkeley National Laboratory, Berkeley, CA, 94720, USA.

E-mail addresses: b.gludovatz@unsw.edu.au (B. Gludovatz), roritchie@lbl.gov (R.O. Ritchie).

sponding tensile stresses remained constant at ~ 720 MPa. This was attributed to the lower yield strength of the Cantor alloy at 293 K relative to 77 K, resulting in a higher strain necessary to achieve the required tensile stress for the onset of twinning [17]. The presumption here is that deformation twinning is a stress-controlled event, given that twinning is known to occur at a 'critical' stress in many alloys [16].

While standard rectangular and cylindrical dogbone-shaped tensile specimens, as used in the studies of Otto et al. [3] and Laplanche et al. [17], are a generally convenient geometry for measuring mechanical properties in tensile tests, they have one major limitation: each sample only allows the measurement and post-test observation of the effect of a single strain state, requiring the preparation of multiple tensile and TEM samples to provide a continuum of data that can correlate microstructure evolution with mechanical properties. Thus, we opted to design and test a dogbone specimen with variable cross-section width and uniform thickness to allow the sampling of multiple stress (strain) states in a single tensile test, thereby simplifying testing procedures and allowing the entire strain range of interest to be sampled in a single specimen, as long as the test is stopped prior to failure. Our intent was to verify both our methodology and the observations of Otto et al. [3] and Laplanche et al. [17] on the occurrence and onset of nano-twinning in CrMnFeCoNi samples deformed in uniaxial tension between ambient temperature and 77 K, to demonstrate that twinning is stress-controlled, and to provide an efficient and meaningful method to screen new alloy compositions for the deformation mechanisms that occur at the individual stress-strain states.

2. Experimental procedures

A 1 kg ingot of the CrMnFeCoNi alloy was produced by vacuum induction melting and cast into a cylindrical steel mold. The ingot was then sealed in an evacuated quartz tube and thermally homogenized at 1473 K for 48 h. Subsequently, the homogenized rod was rotary swaged at room temperature to reduce its diameter from 40 to ~ 16.5 mm before being recrystallized at 1073K for 1 h, yielding a grain size of ~ 7 μm with a random orientation distribution [17]. The rod was then sectioned into planar slices along the longitudinal direction of the rod and machined into modified uniaxial tensile dogbone samples using electrical discharge machining (EDM). A total of 7 samples was machined measuring 28 mm \times 14 mm with a uniform thickness of $t = 2$ mm; the geometry is shown in Fig. 1a.

The faces of all samples were metallographically polished using silicon carbide paper to a final 15 μm surface finish. Post-polishing, one side of the sample was indented along the centerline at intervals of ~ 400 μm using a Vickers microhardness indenter loaded to 300 g; precise locations were documented using an Olympus STM-UM measuring optical microscope (Olympus Corporation, Tokyo, Japan). While these indentations could introduce a small degree of localized deformation and alteration of cross-section, this was deemed to be an insignificant issue whereas the displacements of the indents provided a valuable measure of plastic strain that was conducive to immersion in liquid nitrogen (LN_2).

Due to the non-standard geometry of our specimens, a finite element method (FEM) model was developed using the Osgood-Ramberg plasticity formulation to approximate the localized and global strain experienced by the sample geometry at given loads. Once developed, ABAQUS was used to simulate tensile test runs using this FEM system. These calculations provided the guidelines by which we applied loads to the samples to maximize data acquisition while avoiding extreme plastic deformation such as extensive necking or failure which would make determining the localized strain infeasible. Uniaxial tensile testing was then performed at an extension rate of $1 \mu\text{m s}^{-1}$ using an electro-servo hydraulic MTS testing machine (MTS Corporation, Eden Prairie, MN, USA) controlled by an Instron 8800 digital controller

(Instron Corporation, Norwood, MA, USA).¹ Seven samples were tested at three different temperatures: three samples in air at room temperature (293 K), two immersed in a dry ice/ethanol bath (198 K), and two submerged in LN_2 (77 K).

Post-testing, the final positions of the micro-indentations (that had diagonal lengths of ~ 50 μm) were measured optically with the Olympus STM-UM measuring microscope and the resultant displacements were used to calculate the degree of localized engineering plastic strain along the centerline from which we were able to calculate the localized true plastic strain and average global strains over the length of the sample. (While the sample geometry implies that the stress state within the region of interest is no longer a uniaxial stress state, we assume any error in our estimation to be negligible as a result of the large radius in the necking region of the sample and the only moderate strains applied during testing.) To assist in the characterization of microstructural features such as grain structure and nano-twins, prior to testing the surfaces of the samples were first vibro-polished to a mirror surface finish using a 0.05 μm colloidal silica suspension for 10 h for electron backscatter diffraction (EBSD) imaging and subsequently electropolished for back-scattered electron (BSE) imaging; after testing they were re-polished and additionally electropolished. Initial scanning electron microscopy (SEM) and EBSD imaging was performed using a FEI Strata DB235 SEM (FEI Company, Hillsboro, OR, USA) equipped with a TSL EDAX System (TexSEM Laboratories Inc., Draper, UT, USA) operated at 20 kV with scan step size ranging from 30 to 150 nm to examine grain orientations and deformation twins. Further deformation characterization was conducted using BSE imaging performed on a Zeiss LEO 1525 field-emission scanning electron microscope (FE-SEM, Carl Zeiss, Oberkochen, Germany) operated at 20 kV. For each temperature, 5–12 locations were imaged across the samples tested in those conditions and analyzed to link observed microstructural features with applied local strains.

3. Results and discussion

Prior studies of the CrMnFeCoNi alloy have found evidence of nanoscale deformation twinning after uniaxial tensile or fracture toughness testing at lower temperatures as compared to room temperature tests where twinning was not observed, except at high strains close to failure [3,6,18]. These findings suggest a temperature-dependent threshold strain for the activation of deformation twinning. Using our modified dogbone samples, we sought to corroborate the strain and corresponding activation stress for the onset of nanoscale deformation twinning in this high-entropy alloy, first measured by Laplanche et al. [17], using more tedious TEM methods, by coupling measurement and modeling of localized strains in this geometry with microscopic characterization of the resultant deformation twins.

3.1. Localized strain

After testing, the local engineering plastic strains were calculated from the optical measurements of the displacement of the centerline indentations. Owing to the varying cross-section of the graded dogbone samples, we employed FEM calculations to estimate the corresponding true plastic strains in the sample from the displacement of the indents, as noted above.

Close agreement between the strains calculated from the micro-indentations and modeling methods indicated accurate estimation of the localized and global true strains; the resultant engineering and true strain

¹ The varying width of our modified dogbone geometry naturally results in a gradient of strain rate along the axis of the sample. This variation, however, is relatively minor and would be unlikely to affect the formation of twins or the properties of the material, especially since this alloy has been shown to be relatively insensitive to changes in strain rate [14].

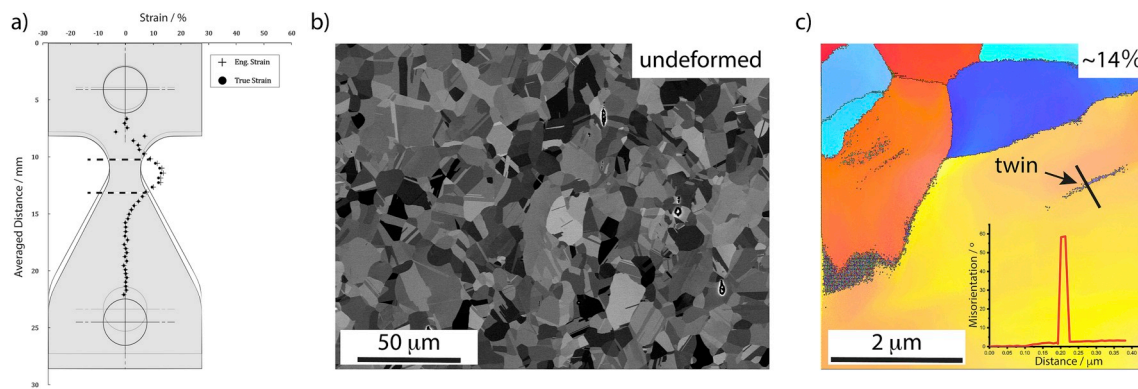


Fig. 1. Localized strain profile and corresponding BSE and EBSD imaging of a CrMnFeCoNi sample tested at 77 K. Engineering and true plastic strain vary with the cross-section of the modified dogbone sample geometry, as shown in **a**) as overlaid schematic of a sample before (white) and after (grey) testing. Dashed black lines indicate the approximate threshold strain values where nano-twinning was predicted, based on data of Laplanche et al. [13]; twinning was thus expected to be observed in the region between these two boundaries. Regions outside of this area, as shown in the BSE image in **b**), reveal a fully recrystallized microstructure with annealing twins. Within the region of the dashed lines, deformation was carried by dislocation motion, as is obvious from color gradients within the individual grains of the EBSD scan in **c**), and nano-scale deformation twinning. Nano-twinning was more frequently observed at larger strains; at smaller strains, such as the $\sim 14\%$ shown in **c**), they were confirmed using misorientation profiles along arbitrarily chosen line paths, as shown from the 60° orientation change in the inset.

Table 1

Summary of strains and corresponding stresses for the onset of deformation twinning in the modified dogbone samples.

Temperature	True maximum sample strain [%]	True maximum sample stress [MPa]	Twinning strain [%]	True twinning stress [MPa]
293 K	4	485	–	–
	34	1034	25	785
	15.4	789	–	–
198 K	13.8	843 ^a	–	–
	40.6	1212	16	742
77 K	44.2	1891	8	635
	12.7	1052	9	841

^a Deformation-induced nano-twinning could not reliably be detected.

curves for one sample are shown in Fig. 1a. Of the seven samples tested, three specimens (two tested at 293 K and one at 198 K) did not exceed the predicted minimum strain threshold required for the onset of deformation twinning at the individual temperatures, as estimated from the work of Laplanche et al. [17]; these samples did not show deformation twinning in the present study as verified by our microstructural analyses. A summary of the tabulated test data can be found in Table 1.

3.2. Microstructural analyses

After testing, all seven samples were re-polished and electropolished on the smooth, un-indented side to examine and characterize the microstructures subjected to different strains. EBSD and BSE imaging were used as complementary characterization techniques: BSE allowed faster, higher resolution imaging to survey and locate twins in the material that may be obscured in the step-size-limited EBSD, while EBSD was primarily used to confirm the identity of visually identified twins by probing the region's angle of misorientation relative to the bulk grain and additionally allowed for the determination of grain orientation (which enabled us to correlate the onset of twinning in individual grains with their corresponding Schmid factor for further characterization). Fig. 1a shows the strain profile of a sample tested in liquid nitrogen and examples of BSE (Fig. 1b) and EBSD (Fig. 1c) images taken from undeformed and deformed regions of samples tested at 77 K; Fig. 2 shows BSE and Fig. 3 EBSD images taken from various

regions of samples tested at the indicated temperatures.

Annealing twins were found within all regions analyzed, consistent with prior microstructural analyses of this alloy [19]; however, the presence of deformation-induced nano-twins was highly location-dependent. BSE imaging of all samples revealed onset thresholds for twinning at (true) plastic strains of $\sim 25\%$ at 293 K (Fig. 2a was taken before the critical stress for the onset of twinning was reached, whereas Fig. 2b was taken above that threshold), $\sim 16\%$ at 198 K, and $\sim 8\%$ at 77 K (Fig. 2c and d shows BSE images taken from regions that showed twinning for both temperatures). This was further supported by EBSD, as shown for the LN₂ tested sample in Fig. 3, where below $\sim 9\%$ strain (Fig. 3a and b) no deformation twins were observed; at $\sim 9\%$ and above this value, however, nano-twins became increasingly obvious (Fig. 3c and d). Table 1 summarizes the strains and corresponding stresses each sample has been tested to at the individual temperatures, and the threshold values where nano-twinning was observed.

These values are remarkably similar to those in Laplanche et al. [17], where the onset of deformation nano-twinning was found to occur at plastic strains of 25% and 7.4% at 293 K and 77 K, respectively, and therefore demonstrate the ease and effectiveness of the graded dogbone geometry for making such measurements.

If nano-twinning is considered to be a stress-induced deformation mechanism, our measurements suggest that the critical (true) stress for the onset of deformation twinning in the Cantor alloy is 750 ± 90 MPa, i.e., not significantly different from the 720 ± 30 MPa range reported previously [13]. Our results of a somewhat larger twinning stress as compared to the findings in Ref. [17] may be correlated with the difference in grain size between $\sim 7 \mu\text{m}$ in this study and $\sim 17 \mu\text{m}$ in the previous study. We believe that any error in our experiments would be small, although some degree of scatter may have resulted from sampling (probing a larger number of regions would enhance the accuracy of our strain estimates), and additional error may have been introduced through the use of micro-indents to mark the surfaces as well as from small deviations from a pure uniaxial stress state.

Finally, it is worth noting that, at room temperature and 77 K, values of 110–140 MPa [20] and 153 MPa [21] have been reported for the critical resolved shear stress for twinning in single crystals of the Cantor alloy. Multiplying these values by the Taylor factor (~ 3) yields tensile twinning stresses of 330–450 MPa, which are lower than those estimated from polycrystalline specimens (720–750 MPa). Among the factors that could account for this discrepancy are (i) orientation dependence of twinning (different grains do not all twin at the same time) and (ii) sampling limitations (TEM foils in Ref. [17] may have missed some

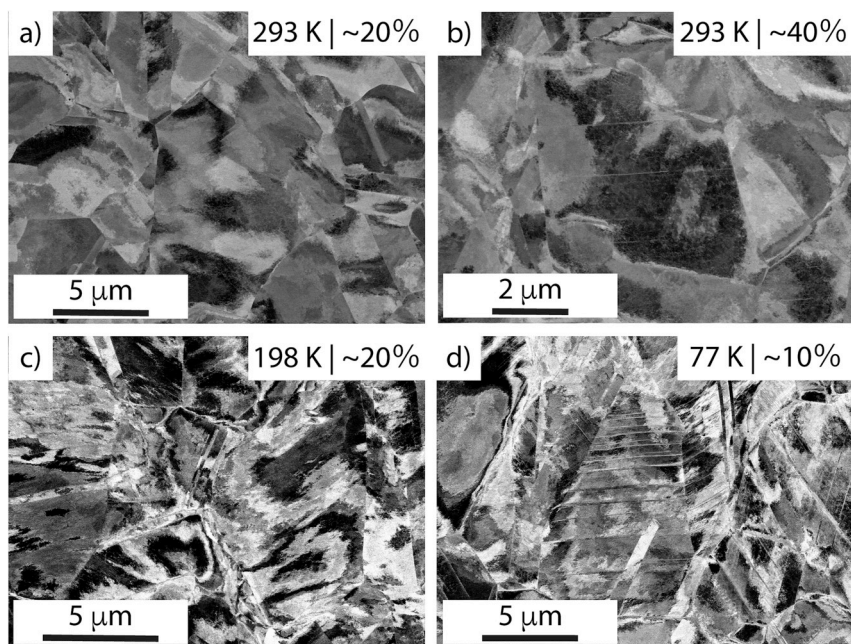


Fig. 2. BSE imaging of localized microstructural deformation of samples tested at 293 K, 198 K, and 77 K. Micrographs taken from samples that were tested at room temperature (a,b) clearly show that a) in regions where the applied strain was not sufficient for the onset of twinning, here ~20%, deformation was carried mainly by dislocation motion, whereas b) above the onset strain required for nano-twinning, deformation twins were observed as additional deformation mode; the sample region shown in b) experienced ~40% strain. At c) 198 K and d) liquid nitrogen temperatures, nano-twinning was obvious at ~20% and ~10% strain, respectively.

twinned grains and EBSD/BSE imaging in the current study can examine only the surface grains). There may also be compositional factors that come into play (through their effects on stacking fault energy) because of potential Mn evaporation during single crystal growth [22] and contamination from the crucible used for single crystal growth.

4. Conclusions

The equiatomic, face-centered cubic, solid-solution CrMnFeCoNi

high-entropy alloy was mechanically tested in uniaxial tension at 293 K, 198 K, and 77 K to determine the onset of nano-twinning in this material. Experiments were conducted using a novel, modified dogbone geometry to allow sampling of regions of varying stresses and strains within a single test specimen. The following conclusions can be drawn:

- The modified uniaxial tensile dogbone specimen provides a reliable method to probe a wide range of stresses and strains within a single specimen allowing efficient determination of the strains and stresses

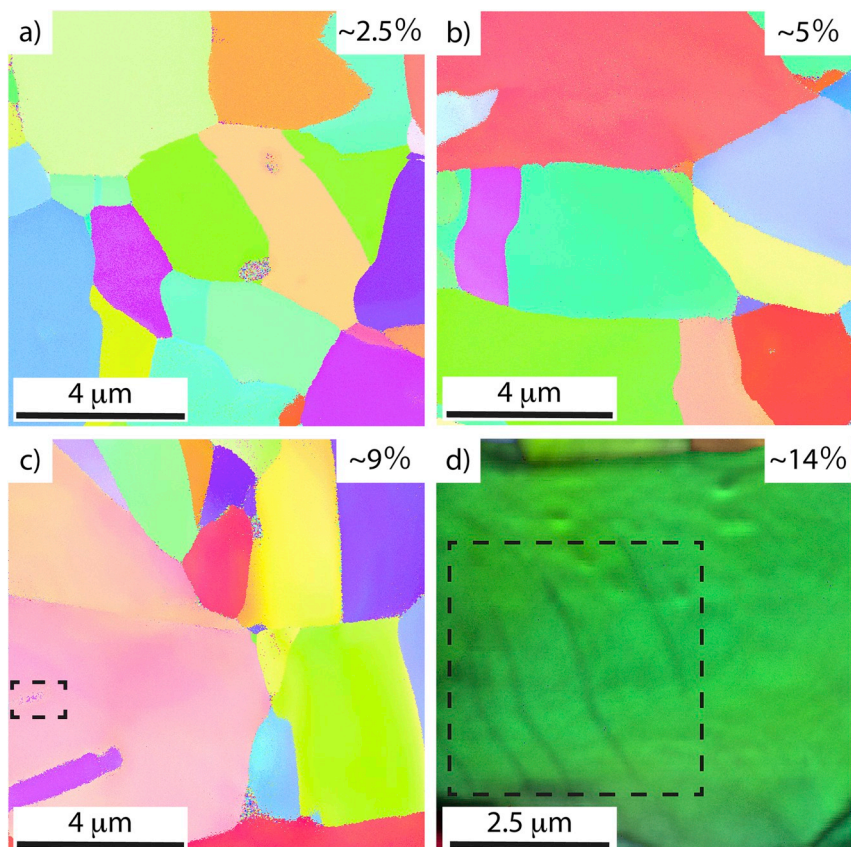


Fig. 3. EBSD imaging of CrMnFeCoNi samples tested at 77 K. EBSD images taken at various positions along the centerline of the sample indicate an increasing propensity for twinning with increasing strain. As shown in a) and b), regions that experienced strains lower than the critical onset strain showed no signs of twinning. Samples that were loaded above this threshold, e.g., ~9% and ~14% true strains, as shown in c) and d), exemplify locations where nano-twinning was observed; they are highlighted with the dashed boxes. (Similar to Fig. 2d, the somewhat bent appearance of the initially straight twins is likely a result of the larger plastic deformation at higher strains.)

for the onset of twinning in this alloy.

- The (true) plastic strains for the onset of nano-twinning were found to be highly temperature dependent: ~25% at 293 K, ~16% at 198 K, and ~8% at 77 K.
- Consistent with the TEM observations of Laplanche et al. [17], these results imply that deformation nano-twinning is stress-dependent with a temperature-independent critical twinning stress of ~750 MPa.

Acknowledgements

This study was supported through the Mechanical Properties of Materials program (KC13) at the Lawrence Berkeley National Laboratory (LBNL) by the U.S. Department of Energy, Office of Science, Office of Basic Energy Sciences, under contract no. DE-AC02-05-CH11231 (KVST, BG, ROR). E.P.G. was supported by the U.S. Department of Energy, Office of Science, Basic Energy Sciences, Materials Sciences and Engineering Division. G.L. acknowledges funding from the German Research Foundation (DFG) through project LA 3607/1-1, and KVST for an NSF Graduate Fellowship from NSF GRFP grant no. 1106400. The authors additionally thank Mr. Caleb Boyd for assistance with mechanical testing, Dr. Joseph McKeown for help in microstructural characterization, and Dr. Ashvini Shekhawat for the numerical analysis.

References

- [1] B. Cantor, I.T.H. Chang, P. Knight, A.J.B. Vincent, Microstructural development in equiatomic multicomponent alloys, *Mater. Sci. Eng. A* 375–377 (2004) 213–218, <https://doi.org/10.1016/j.msea.2003.10.257>.
- [2] B. Gludovatz, A. Hohenwarter, D. Catoor, E.H. Chang, E.P. George, R.O. Ritchie, A fracture-resistant high-entropy alloy for cryogenic applications, *Science* 345 (2014) 1153–1158, <https://doi.org/10.1126/science.1254581>.
- [3] F. Otto, A. Dlouhý, C. Somsen, H. Bei, G. Eggeler, E.P. George, The influences of temperature and microstructure on the tensile properties of a CoCrFeMnNi high-entropy alloy, *Acta Mater.* 61 (2013) 5743–5755, <https://doi.org/10.1016/j.actamat.2013.06.018>.
- [4] N. Stepanov, M. Tikhonovsky, N. Yurchenko, D. Zyabkin, M. Klimova, S. Zherebtsov, A. Efimov, G. Salishchev, Effect of cryo-deformation on structure and properties of CoCrFeNiMn high-entropy alloy, *Intermetallics* 59 (2015) 8–17, <https://doi.org/10.1016/j.intermet.2014.12.004>.
- [5] F. Otto, Y. Yang, H. Bei, E.P. George, Relative effects of enthalpy and entropy on the phase stability of equiatomic high-entropy alloys, *Acta Mater.* 61 (2013) 2628–2638, <https://doi.org/10.1016/j.actamat.2013.01.042>.
- [6] B. Gludovatz, E.P. George, R.O. Ritchie, Processing, microstructure and mechanical properties of the CrMnFeCoNi high-entropy alloy, *JOM* 67 (2015) 2262–2270, <https://doi.org/10.1007/s11837-015-1589-z>.
- [7] V. Shterner, I.B. Timokhina, H. Beladi, On the work-hardening behaviour of a high manganese TWIP steel at different deformation temperatures, *Mater. Sci. Eng. A* 669 (2016) 437–446, <https://doi.org/10.1016/j.msea.2016.05.104>.
- [8] X.-H. Fang, P. Yang, F.-Y. Lu, L. Meng, Dependence of deformation twinning on grain orientation and texture evolution of high manganese TWIP steels at different deformation temperatures, *J. Iron Steel Res. Int.* 18 (2011) 46–52, [https://doi.org/10.1016/S1006-706X\(11\)60116-7](https://doi.org/10.1016/S1006-706X(11)60116-7).
- [9] V. Shterner, A. Molotnikov, I. Timokhina, Y. Estrin, H. Beladi, A constitutive model of the deformation behaviour of twinning induced plasticity (TWIP) steel at different temperatures, *Mater. Sci. Eng. A* 613 (2014) 224–231, <https://doi.org/10.1016/j.msea.2014.06.073>.
- [10] X. Fu, X. Wu, Q. Yu, Dislocation plasticity reigns in a traditional twinning-induced plasticity steel by in situ observation, *Mater. Today Nano* 3 (2018) 48–53, <https://doi.org/10.1016/j.mtnano.2018.11.004>.
- [11] Y. Li, Y. Lu, W. Li, M. Khedr, H. Liu, X. Jin, Hierarchical microstructure design of a bimodal grained twinning-induced plasticity steel with excellent cryogenic mechanical properties, *Acta Mater.* 158 (2018) 79–94, <https://doi.org/10.1016/j.actamat.2018.06.019>.
- [12] A.J. Zaddach, C. Niu, C.C. Koch, D.L. Irving, Mechanical properties and stacking fault energies of NiFeCrCoMn high-entropy alloy, *JOM* 65 (2013) 1780–1789, <https://doi.org/10.1007/s11837-013-0771-4>.
- [13] M.A. Meyers, O. Vöhringer, V.A. Lubarda, The onset of twinning in metals: a constitutive description, *Acta Mater.* 49 (2001) 4025–4039, [https://doi.org/10.1016/S1359-6454\(01\)00300-7](https://doi.org/10.1016/S1359-6454(01)00300-7).
- [14] G. Laplanche, J. Bonneville, C. Varvenne, W.A. Curtin, E.P. George, Thermal activation parameters of plastic flow reveal deformation mechanisms in the CrMnFeCoNi high-entropy alloy, *Acta Mater.* 143 (2018) 257–264, <https://doi.org/10.1016/j.actamat.2017.10.014>.
- [15] Z. Wu, C.M. Parish, H. Bei, Nano-twin mediated plasticity in carbon-containing FeNiCoCrMn high entropy alloys, *J. Alloy. Comp.* 647 (2015) 815–822, <https://doi.org/10.1016/j.jallcom.2015.05.224>.
- [16] B. Gludovatz, A. Hohenwarter, K.V.S. Thurston, H. Bei, Z. Wu, E.P. George, R.O. Ritchie, Exceptional damage-tolerance of a medium-entropy alloy CrCoNi at cryogenic temperatures, *Nat. Commun.* 7 (2016) 10602, <https://doi.org/10.1038/ncomms10602>.
- [17] G. Laplanche, A. Kostka, O.M. Horst, G. Eggeler, E.P. George, Microstructure evolution and critical stress for twinning in the CrMnFeCoNi high-entropy alloy, *Acta Mater.* 118 (2016) 152–163, <https://doi.org/10.1016/j.actamat.2016.07.038>.
- [18] K.V.S. Thurston, B. Gludovatz, A. Hohenwarter, G. Laplanche, E.P. George, R.O. Ritchie, Effect of temperature on the fatigue-crack growth behavior of the high-entropy alloy CrMnFeCoNi, *Intermetallics* 88 (2017) 65–72, <https://doi.org/10.1016/j.intermet.2017.05.009>.
- [19] F. Otto, N.L. Hanold, E.P. George, Microstructural evolution after thermo-mechanical processing in an equiatomic, single-phase CoCrFeMnNi high-entropy alloy with special focus on twin boundaries, *Intermetallics* 54 (2014) 39–48, <https://doi.org/10.1016/j.intermet.2014.05.014>.
- [20] I.V. Kireeva, Y.I. Chumlyakov, Z.V. Pobedennaya, I.V. Kuksgausen, I. Karaman, Orientation dependence of twinning in single crystalline CoCrFeMnNi high-entropy alloy, *Mater. Sci. Eng. A* 705 (2017) 176–181, <https://doi.org/10.1016/j.msea.2017.08.065>.
- [21] W. Abuzaid, H. Sehitoglu, Critical resolved shear stress for slip and twin nucleation in single crystalline FeNiCoCrMn high entropy alloy, *Mater. Char.* 129 (2017) 288–299, <https://doi.org/10.1016/j.matchar.2017.05.014>.
- [22] S. Haas, M. Mosbacher, O.N. Senkov, M. Feuerbacher, J. Freudenberger, S. Gezgin, R. Völkl, U. Glatzel, Entropy determination of single-phase high entropy alloys with different crystal structures over a wide temperature range, *Entropy* 20 (2018) 654, <https://doi.org/10.3390/e20090654>.